© 2017. Published by The Company of Biologists Ltd | Journal of Cell Science (2017) 130, 2606-2619 doi:10.1242/jcs.194563

RESEARCH ARTICLE

The cell adhesion molecule CHL1 interacts with patched-1 to regulate apoptosis during postnatal cerebellar development

Jelena Katic[1], Gabriele Loers[1], Jelena Tosic[1], Melitta Schachner[2,3,4,*] and Ralf Kleene[1]

ABSTRACT

The immunoglobulin superfamily adhesion molecule close homolog of L1 (CHL1) plays important roles during nervous system development. Here, we identified the hedgehog receptor patched-1 (PTCH1) as a novel CHL1-binding protein and showed that CHL1 interacts with the first extracellular loop of PTCH1 via its extracellular domain. Colocalization and co-immunoprecipitation of CHL1 with PTCH1 suggest an association of CHL1 with this major component of the hedgehog signaling pathway. The *trans*-interaction of CHL1 with PTCH1 promotes neuronal survival in cultures of dissociated cerebellar granule cells and of organotypic cerebellar slices. An inhibitor of the PTCH1-regulated hedgehog signal transducer, smoothened (SMO), and inhibitors of RhoA and Rho-associated kinase (ROCK) 1 and 2 prevent CHL1-dependent survival of cultured cerebellar granule cells and survival of cerebellar granule and Purkinje cells in organotypic cultures. In histological sections from 10- and 14-day-old CHL1-deficient mice, enhanced apoptosis of granule, but not Purkinje, cells was observed. The results of the present study indicate that CHL1 triggers PTCH1-, SMO-, RhoA- and ROCK-dependent signal transduction pathways to promote neuronal survival after cessation of the major morphogenetic events during mouse cerebellar development.

KEY WORDS: CHL1, Patched-1, Smoothened, Apoptosis, Signal transduction, Cerebellar development

INTRODUCTION

Cell adhesion molecules regulate neural cell proliferation, migration, differentiation and survival (Maness and Schachner, 2007). The cell adhesion molecule CHL1 (Holm et al., 1996; Hillenbrand et al., 1999) contributes to these developmental events, and ablation of CHL1 in mice results in malformation of brain structures (Montag-Sallaz et al., 2002; Demyanenko et al., 2004, 2011; Nikonenko et al., 2006; Wright et al., 2007; Ango et al., 2008; Jakovcevski et al., 2009). In the cerebellum, CHL1 deficiency leads to aberrant branching, orientation and targeting of cerebellar stellate cell axons as well as loss of cerebellar Purkinje and granule cells (Ango et al., 2008; Jakovcevski et al., 2009).

The functions of CHL1 are diverse; CHL1 reduces proliferation and differentiation of neural progenitor cells (Huang et al., 2011; Katic et al., 2014), but promotes survival and migration of differentiated neural cells (Holm et al., 1996; Chen et al., 1999; Hillenbrand et al., 1999; Buhusi et al., 2003; Jakovcevski et al., 2007, 2009; Katic et al., 2014). Moreover, CHL1 regulates neuritogenesis through different mechanisms (Chen et al., 1999; Hillenbrand et al., 1999; Jakovcevski et al., 2007, 2009; Katic et al., 2014). In search for novel binding partners for CHL1, we found that PTCH1 and CHL1 associate in a heterophilic *trans*-interaction. The 12-pass transmembrane protein PTCH1 is a cognate receptor for the three mammalian hedgehog family members sonic hedgehog (SHH), desert hedgehog (DHH) and indian hedgehog (IHH), which act as morphogens and function as signaling molecules by binding to PTCH1 (for reviews and references therein, see Jenkins, 2009; Robbins et al., 2012; Briscoe and Thérond, 2013). PTCH1 represses the seven-pass transmembrane G protein-coupled receptor SMO, and binding of hedgehog proteins to PTCH1 leads to dissociation of SMO from PTCH1 and to relief of SMO repression by PTCH1. In the so-called 'canonical' hedgehog signaling pathway, binding of hedgehog ligands to PTCH1 activates SMO which, in turn, activates the transcription factors glioma-associated oncogene 1, 2 and/or 3 (Gli-1, -2, -3) which regulate the expression of a number of effector genes, including the *PTCH1* gene (Goodrich et al., 1997; Robbins et al., 2012; Briscoe and Thérond, 2013). PTCH1 mediates also 'non-canonical' SMO-dependent and -independent hedgehog signaling through Gli-independent mechanisms. Furthermore, PTCH1 also functions as a 'dependence-receptor': in the absence of hedgehog ligands, PTCH1 induces apoptosis after cleavage of the seventh cytoplasmic C-terminal PTCH1 domain by caspase-3 (Thibert et al., 2003; Mille et al., 2009; Fombonne et al., 2012).

Having found CHL1 to be a novel binding partner for PTCH1, in the present study, we investigated the functional consequences of this interaction in cellular and molecular terms during mouse cerebellar development.

RESULTS

CHL1 interacts with PTCH1

In search for proteins that bind to the extracellular part of CHL1 which comprises six immunoglobulin-like (Ig-like) domains, four fibronectin type III (FNIII) domains and one partial FNIII domain (Holm et al., 1996) (Fig. 1A), we used a recombinant fusion protein of the extracellular CHL1 domains and human Fc (CHL1–Fc) to screen a phage-display peptide library. Out of 20 CHL1–Fc-binding phages, 15 phages expressed a peptide sequence that showed similarity to a sequence stretch in the first extracellular loop of PTCH1 (Fig. 1B). As an initial step to support the notion that CHL1 binds to PTCH1, we performed immunoprecipitation experiments with detergent extracts of brains from wild-type or CHL1-deficient mice using anti-CHL1 antibody and, for control, antibodies against the immunoglobulin superfamily adhesion molecules L1 (L1CAM, hereafter denoted L1) and NCAM1 (hereafter denoted NCAM). In the subsequent western blot analyses, PTCH1 was detected in CHL1 immunoprecipitates from wild-type mice, but not from

[1]Zentrum für Molekulare Neurobiologie, Universitätsklinikum Hamburg-Eppendorf, Martinistr. 52, 20246 Hamburg, Germany. [2]Keck Center for Collaborative Neuroscience, Rutgers University, 604 Allison Road, Piscataway, NJ 08854, USA. [3]Department of Cell Biology and Neuroscience, Rutgers University, 604 Allison Road, Piscataway, NJ 08854, USA. [4]Center for Neuroscience, Shantou University Medical College, 22 Xin Ling Road, Shantou, Guangdong 515041, China.

*Author for correspondence (schachner@stu.edu.cn)

G.L., 0000-0003-1851-562X; J.T., 0000-0003-0043-1460; M.S., 0000-0001-8561-9037; R.K., 0000-0002-5935-5266

Received 30 June 2016; Accepted 13 June 2017

Journal of Cell Science (2017) 130, 2606-2619 doi:10.1242/jcs.194563

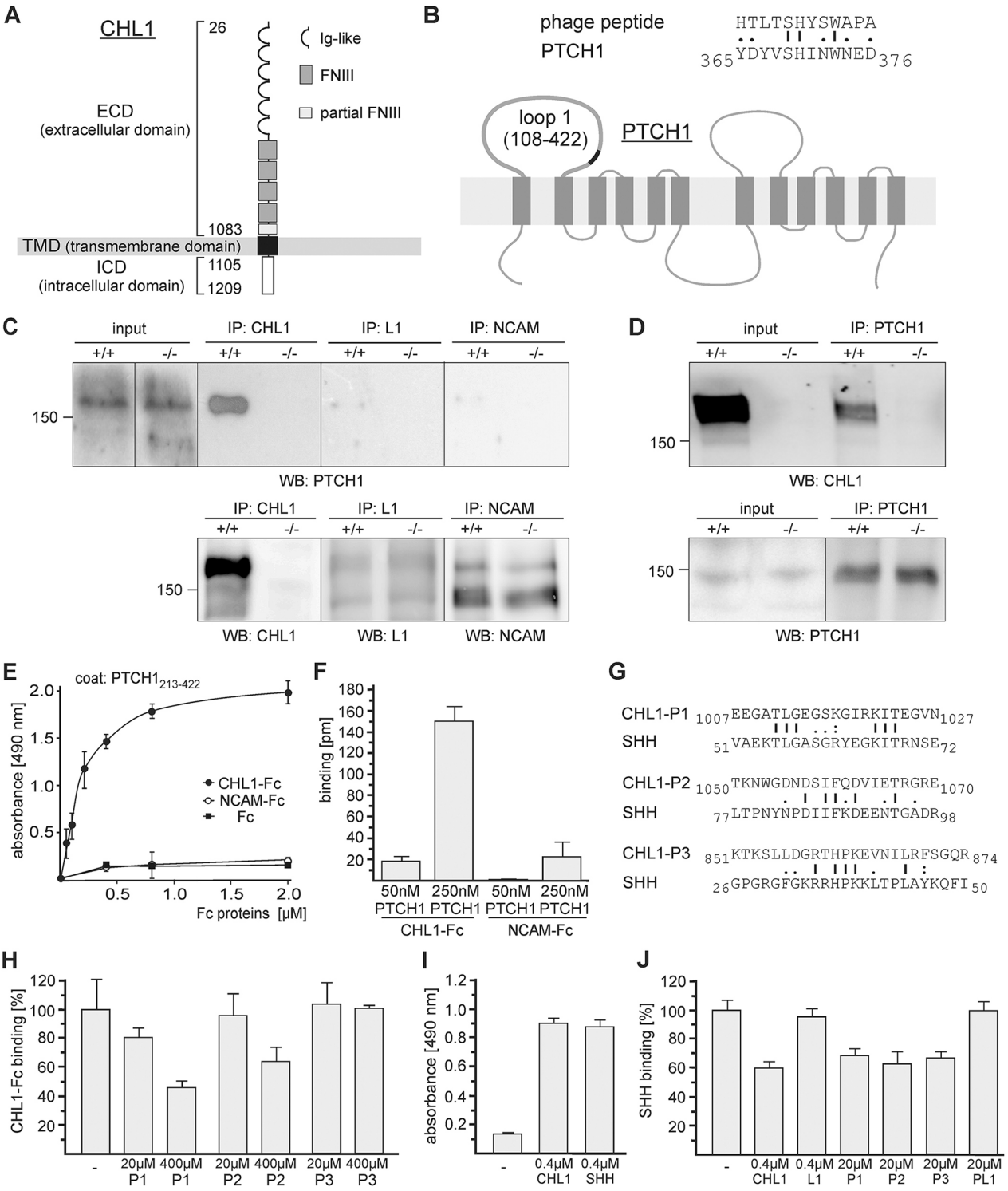

Fig. 1. CHL1 interacts with PTCH1. (A,B) The schemes show the membrane topology structure of CHL1 and PTCH1 (amino acid positions are indicated). (B) The peptide sequence that was identified in the phages binding to CHL1–Fc is similar to a sequence in loop 1 of PTCH1. (C,D) Homogenates of brains (C) or cerebella (D) from 14-day-old CHL1-deficient (CHL1 –/–) and wild-type (CHL1 +/+) mice were subjected to immunoprecipitation (IP) followed by western blot analysis (WB) using antibodies against CHL1, L1, NCAM or PTCH1. (E) Mean±s.d. values from three independent experiments with triplicates are shown for binding in ELISA using a substrate-coated PTCH1 fragment and increasing concentrations of CHL1–Fc, NCAM–Fc or Fc. (F) Mean±s.d. values of reflected wavelength shifts in pm from three independent experiments each performed in triplicate are shown for the label-free binding assay using substrate-coated CHL1–Fc, NCAM-Fc and Fc and 50 nM or 250 nM PTCH1 fragment in solution. (G) CHL1-derived peptides CHL1-P1, -P2 and -P3 show sequence similarities to SHH. (H–J) Substrate-coated PTCH1 was incubated without (–) or with 400 nM CHL1–Fc in the absence (–) or presence of 20 μM or 400 μM CHL1-P1, -P2 or -P3 (H), or with 400 nM CHL1–Fc or SHH (I), or with 400 nM SHH in the absence (–) or presence of 400 nM CHL1–Fc or L1–Fc or of 20 μM CHL1-P1, -P2 or -P3 or L1-derived peptide PL1 (J). Mean±s.d. values from three independent experiments each carried out in triplicates are shown for the binding of CHL1–Fc or SHH to the PTCH1 fragment in the presence of peptides relative to the binding in their absence (set to 100%). In B and G, amino acid positions, and identical (|), highly conserved (:) or weakly conserved (.) amino acids are indicated.

Journal of Cell Science

Journal of Cell Science (2017) 130, 2606-2619 doi:10.1242/jcs.194563

CHL1-deficient mice (Fig. 1C). Only very low levels of PTCH1 were seen in L1 and NCAM immunoprecipitates from wild-type mice, with no PTCH1 seen in L1 and NCAM immunoprecipitates from CHL1-deficient mice (Fig. 1C), suggesting that a very small portion of CHL1 unspecifically binds to the beads and co-precipitates very small amounts of PTCH1. CHL1 appeared as an ∼185 kDa band in CHL1 immunoprecipitates from wild-type, but not CHL1-deficient, brains (Fig. 1C). Similar levels of the ∼200 and ∼140 kDa L1 protein forms and the ∼140 and ∼180 kDa NCAM isoforms were observed in L1 and NCAM immunoprecipitates, respectively, from wild-type and CHL1-deficient brains (Fig. 1C). When using detergent extracts of cerebella from wild-type and CHL1-deficient mice for immunoprecipitation with anti-PTCH1 antibody, CHL1 was found in PTCH1 immunoprecipitates from cerebella of wild-type mice, but not of CHL1-deficient, mice (Fig. 1D). Similar amounts of PTCH1 were observed in detergent extracts and PTCH1 immunoprecipitates from wild-type and CHL1-deficient cerebella (Fig. 1D). These results support the notion that CHL1 associates with PTCH1.

To test for a direct interaction between CHL1 and PTCH1, ELISA experiments were performed using increasing concentrations of CHL1–Fc, NCAM–Fc or Fc and a substrate-coated recombinant PTCH1 protein fragment which contains part of the first extracellular loop and the putative CHL1-binding site. A concentration-dependent binding of CHL1–Fc, but not NCAM–Fc or Fc, to PTCH1 was observed (Fig. 1E), showing that CHL1 and PTCH1 interact via their extracellular domains. An alternative method to show direct interaction, a label-free binding assay was performed, which showed the direct interaction of the PTCH1 fragment to immobilized CHL1–Fc, but not to NCAM–Fc (Fig. 1F).

Since CHL1 appears to represent a PTCH1 ligand that is like the ‘canonical’ PTCH1 ligands SHH, DHH and IHH, we searched for sequence similarities between CHL1 and hedgehog family members to identify putative binding sites for PTCH1 in CHL1. Amino acids 851–874, 1007–1027 and 1050–1070 in the third, fourth and partial FNIII domain of murine CHL1 (Holm et al., 1996) were similar in sequence to amino acids 26–50, 51–72 and 77–98, respectively, in the N-terminal domain of murine SHH, but not DHH and IHH. Interestingly, CHL1 and SHH sequences from several vertebrate species displayed three common motifs: TLGxxxK/RxxxKIT/S, DxIFxDxxxT and RxHPKxxxxL (Fig. 1G). Synthetic CHL1-derived peptides containing these motifs were used as competitors in ELISA with PTCH1 protein fragment and CHL1–Fc. At high concentrations, the peptides containing the TLGxxxK/RxxxKIT/S or DxIFxDxxxT motif, but not the peptide with the RxHPKxxxxL motif, interfered with the binding of CHL1–Fc to the substrate-coated PTCH1 fragment (Fig. 1H).

Next, we analyzed whether SHH also binds to the recombinant PTCH1 protein fragment containing the first extracellular loop and asked whether CHL1–Fc and/or the CHL1-derived peptides compete with this binding. SHH and CHL1–Fc bound to PTCH1 with similar efficiency (Fig. 1I), and the binding of SHH to the PTCH1 loop was reduced by equimolar concentrations of CHL1–Fc, but not by L1–Fc (Fig. 1J), indicating that CHL1 and SHH compete for binding to the first extracellular loop of PTCH1. Notably, all CHL1-derived peptides, but not a L1-derived control peptide, interfered with the binding of SHH to substrate-coated PTCH1 protein at low micromolar concentrations (Fig. 1J).

CHL1 colocalizes with PTCH1 in the developing cerebellar cortex

To investigate whether CHL1 is associated with PTCH1 in cerebellar tissue, immunostainings of cerebellar slices of 7-day-old mice were performed, and these showed a considerable colocalization in the molecular layer and on cells in the internal granular layer of wild-type mice (Fig. 2A,B), but not CHL1-deficient mice (Fig. 2C).

To further investigate these associations, we used anti-PTCH1 and -CHL1 antibodies in a proximity ligation assay, which allows sensitive detection of molecular interactions by amplification of fluorescent signals from a pair of oligonucleotide-labeled secondary antibodies if the primary antibodies bind to their antigens in close proximity (<40 nm). Many fluorescent spots were found in the molecular and internal granular layers of cerebella from 7-, 10- and 14-day-old wild-type mice, and in the innermost external granule layer of cerebella from 7- and 10-day-old wild-type mice (Fig. 3A–C). No fluorescent signals were detectable in sections of 7-day-old CHL1-deficient mice with anti-CHL1 and -PTCH1 antibodies (Fig. 3D) or in sections of 7-day-old wild-type mice using anti-PTCH1 antibody alone (Fig. 3E) or using antibodies against CHL1 and SHH (Fig. 3F), which is also expressed in the cerebellum. This result excludes the possibility that unspecific fluorescent signals arise from detection of CHL1 and PTCH1 alone. In summary, our results indicate close interactions of CHL1 with PTCH1 in postnatally developing cerebellum.

Binding of CHL1 to PTCH1 prevents PTCH1-induced neuronal cell death via a SMO-dependent pathway

Since overexpression of PTCH1 in HEK293 cells leads to enhanced cell death that is reduced to basal levels by application of SHH, showing that PTCH1 is a ‘dependence receptor’ (Thibert et al., 2003), and since CHL1 binds to PTCH1 and promotes cell survival (Chen et al., 1999; Jakovcevski et al., 2009), we tested whether CHL1 acts as PTCH1 ligand to reduce PTCH1-triggered cell death. To this aim, CHL1–Fc and, as a control, L1–Fc was applied to PTCH1-overexpressing HEK293 cells. In comparison to mock-transfected cells, cell death was increased in transfected cells overexpressing PTCH1, while addition of CHL1–Fc, but not L1–Fc, to PTCH1-overexpressing cells inhibited this enhanced cell death (Fig. 4A,B). In contrast, CHL1–Fc did not affect cell death induced by the dependence receptor deleted in colorectal cancer (DCC) (Mehlen et al., 1998) (Fig. 4C), indicating that CHL1 specifically inhibits PTCH1-induced cell death. Since PTCH1 regulates the SMO-dependent signal transduction pathway (Charron and Tessier-Lavigne, 2005), we tested whether CHL1–Fc promotes cell survival via SMO-dependent signaling and analyzed whether the CHL1–Fc-enhanced cell survival was affected by the SMO antagonist SANT-1, which directly binds to SMO (Chen et al., 2002; Rominger et al., 2009; Stanton and Peng, 2010). As control, the inactive SMO antagonist tomatidine (Rominger et al., 2009) was used. In the combined presence of CHL1 and SANT-1, but not tomatidine, CHL1–Fc-induced reduction of cell death was abolished, while SANT-1 and tomatidine did not affect the PTCH1-induced cell death in the absence of CHL1–Fc (Fig. 4B). These results demonstrate that the binding of CHL1 to PTCH1 prevents PTCH1-induced cell death in a SMO-dependent manner. Since CHL1 binds to sequence stretches in the first extracellular loop of PTCH1 (see Fig. 1E), we tested whether binding of CHL1 to this PTCH1 loop prevents PTCH1-induced cell death by using a PTCH1 mutant with a deletion of the first extracellular loop. Through cell surface biotinylation and western blot analysis of isolated biotinylated proteins with anti-PTCH1 antibody, we ensured that full-length and truncated PTCH1 proteins were expressed at the surface of HEK293 cells, which showed a very weak endogenous expression of PTCH1 (Fig. 4D). HEK293 cells expressing full-length PTCH1 and

Journal of Cell Science (2017) 130, 2606-2619 doi:10.1242/jcs.194563

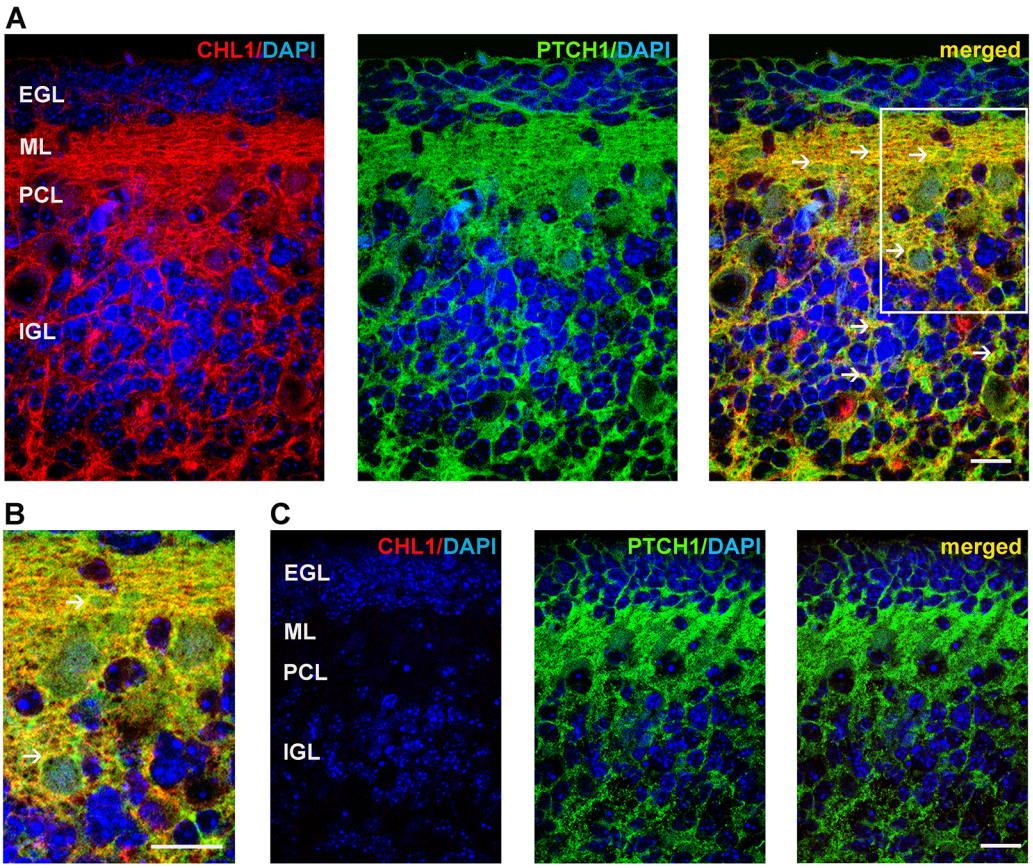

Fig. 2. Association of CHL1 with PTCH1 in the 7-day-old cerebellum. Representative images of immunostaining for CHL1 (red) and PTCH1 (green) in cerebellar sections from 7-day-old wild-type (A,B) and CHL1-deficient (C) mice are shown. Nuclei are stained with DAPI (blue). Superimposition indicates colocalization in yellow (arrows). The box in A (right image) indicates the region shown in a magnified view in B. EGL, external granular layer; ML, molecular layer; PCL, Purkinje cell layer; IGL, internal granular layer. Scale bars: 15 µm.

cells expressing the PTCH1 deletion mutant showed similar levels of cell death (Fig. 4E), indicating that the first extracellular PTCH1 loop is not required for the induction of cell death. However, application of CHL1–Fc did not prevent cell death induced by the PTCH1 mutant, in contrast to the CHL1–Fc-triggered prevention of cell death induced by non-mutated full-length PTCH1 (Fig. 4E), showing that the binding of CHL1 to the first extracellular PTCH1 loop prevents PTCH1-induced cell death.

Since cleavage of the C-terminal PTCH1 domain by caspase-3 in the absence of PTCH1 ligands is required for PTCH1-induced cell death (Thibert et al., 2003), PTCH1-enhanced cell death was measured in the absence of CHL1 to investigate whether this cell death is associated with enhanced caspase-3 activity and whether CHL1–Fc application affects the activity of this caspase. Since binding of SHH to PTCH1 leads to a reduction of PTCH1-enhanced caspase-3 activity and thus to reduced cell death independently of SMO (Thibert et al., 2003), we analyzed in parallel the effect of SHH on caspase-3 activity. Relative to mock-transfected HEK293 cells, caspase-3 activity was increased in PTCH1-overexpressing cells (Fig. 4F). This elevated activity was reduced by addition of CHL1–Fc in the absence and presence of tomatidine, but not in the presence of SANT-1 (Fig. 4F). The enhanced caspase-3 activity was not affected by L1–Fc or by SANT-1 in the absence of CHL1–Fc (Fig. 4F). PTCH1-enhanced caspase-3 activity was also reduced by SHH, but SANT-1 had no effect on the reduction of caspase-3 activity by SHH (Fig. 4F). These results suggest that the binding of CHL1 to PTCH1 inhibits caspase-3-mediated PTCH1 cleavage and PTCH1-induced cell death via SMO-dependent signaling pathways, while binding of SHH to PTCH1 prevents caspase-3-mediated PTCH1 cleavage and PTCH1-induced cell death in a SMO-independent manner. Western blot analysis with an anti-SMO antibody showed that HEK293 cells express SMO (Fig. 4G).

Based on the finding that cell death of CHL1-deficient cerebellar granule cells is increased and abolished by CHL1–Fc (Jakovcevski et al., 2009) and since PTCH1 is an apoptosis-inducing 'dependence receptor' in the absence of its ligands, we investigated whether CHL1–Fc can reduce cell death of CHL1-deficient cerebellar neurons via binding to PTCH1 and activation of SMO-dependent pathways. To this aim, CHL1-deficient cerebellar granule cells were maintained in culture for 5 days and then subjected to serum-deprivation for 2 days in the absence or presence of CHL1–Fc or, as control, L1–Fc and with or without SANT-1 or tomatidine. In parallel, neurons were serum-deprived in the presence of the SMO agonist SAG (Chen et al., 2002) and of SHH alone or together with SANT-1. When compared to cell death induced by serum deprivation in the absence of CHL1, cell death was reduced by CHL1–Fc (Fig. 5A). The reduction in cell death by CHL1–Fc was concentration-dependent and saturable (Fig. 5B). SAG and CHL1–Fc inhibited PTCH1-induced cell death to a similar extent (Fig. 5C), while L1–Fc did not affect PTCH1-induced cell death (Fig. 5D). Reduction of cell death by CHL1–Fc was abolished by SANT-1, but not by tomatidine, while neither SANT-1 nor tomatidine changed cell death levels in the absence of CHL1–Fc (Fig. 5D). Interestingly, SHH did not influence cell death in absence

Journal of Cell Science (2017) 130, 2606-2619 doi:10.1242/jcs.194563

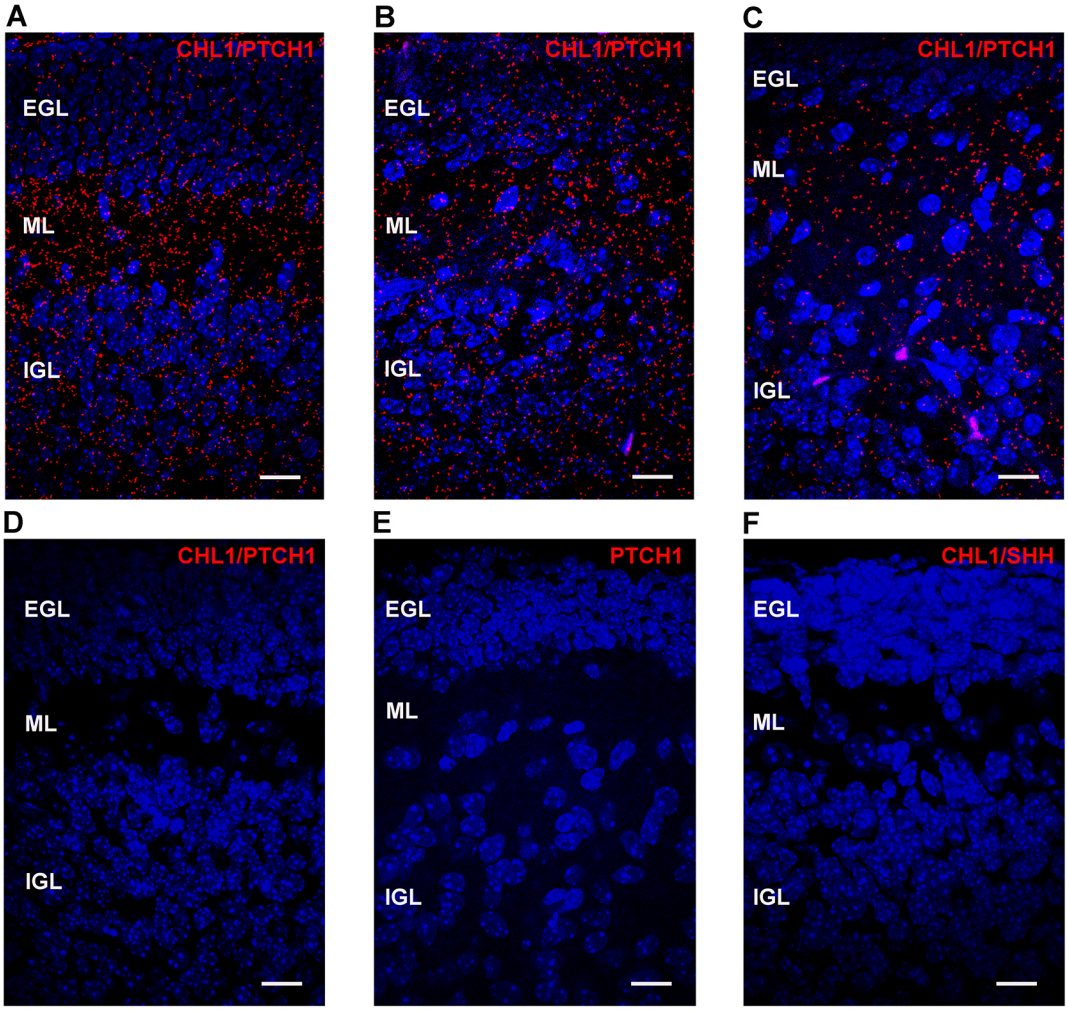

Fig. 3. Colocalization of CHL1 with PTCH1 at different postnatal stages of cerebellar development. Cerebellar sections from 7- (A,D,E,F), 10- (B) and 14-day-old (C) wild-type (A–C,E,F) and CHL1-deficient (D) mice were analyzed with a proximity ligation assay using anti-CHL1 and -PTCH1 antibodies (A–D), anti-PTCH1 antibody alone (E) or anti-CHL1 and -SHH antibodies (F). Representative images are shown, and red spots indicate close interaction of CHL1 with PTCH1 (A–C) in wild-type mice. Nuclei are stained with DAPI (blue). EGL, external granular layer; ML, molecular layer; IGL, internal granular layer. Scale bars: 15 µm.

or presence of SANT-1 (Fig. 5D). These results indicate that binding of CHL1 to PTCH1 promotes cell survival in a SMO-dependent manner, while binding of SHH alone does not alter cell survival of cerebellar granule cells upon serum deprivation.

To further substantiate that CHL1 prevents PTCH1-induced apoptosis of cerebellar granule cells by binding to PTCH1, we asked whether CHL1-induced survival of CHL1-deficient cerebellar granule cells could be blocked by an antibody directed against amino acids 108–422 of the first extracellular loop of PTCH1. Promotion of cell survival by CHL1–Fc was inhibited by this antibody, but not by a non-immune control antibody (Fig. 5E). This result indicates that CHL1 promotes cell survival via binding to PTCH1.

Next, we tested whether the CHL1-derived peptides containing putative PTCH1-binding motifs (see Fig. 1G) could interfere with the CHL1–Fc-triggered prevention of cell death. In the presence of the peptide containing the TLGxxxK/RxxxKIT/S motif, CHL1–Fc-triggered cell survival was found to be abolished, but it was unaltered in the presence of peptides with the DxIFxDxxxT or RxHPKxxxxL motif (Fig. 5F). This result suggests that amino acids 1007–1027 of CHL1 containing the TLGxxxK/RxxxKIT/S motif mediate the interaction of CHL1 with PTCH1 to prevent PTCH1-induced cell death.

Since PTCH1-induced cell death in the absence of PTCH1 ligands requires cleavage of PTCH1 by caspase-3 and PTCH1-dependent activation of caspase-9 (Thibert et al., 2003; Mille et al., 2009; Fombonne et al., 2012), we asked whether CHL1–Fc affects caspase-3 and -9 activities in CHL1-deficient cerebellar granule cells via PTCH1/SMO-dependent pathways. Relative to the caspase-3 and -9 activity levels in the absence of CHL1–Fc, reduced levels were observed after application of CHL1–Fc, but not after application of L1–Fc (Fig. 5G,H). SANT-1 inhibited the CHL1-induced reduction of caspase-3 and caspase-9 activity (Fig. 5G,H). In the presence of CHL1–Fc, caspase-3 and -9 activities were not changed by tomatidine (Fig. 5G,H). These results indicate that binding of CHL1 to PTCH1 inhibits the PTCH1-induced activation of caspase-9 and caspase-3 via a SMO-dependent mechanism, resulting in the prevention of PTCH1-induced cell death.

While in the first postnatal week, cerebellar granule cell numbers are the same in wild-type and CHL1-deficient mice, loss of granule cells is observed in the cerebellum of 2-month-old CHL1-deficient mice (Jakovcevski et al., 2009). In the present study, application of CHL1–Fc to dissociated neurons from 7-day-old CHL1-deficient mice inhibited cell death induced by serum-deprivation for 2 days after 5 days in culture with serum via a SMO-dependent pathway. We

Journal of Cell Science (2017) 130, 2606-2619 doi:10.1242/jcs.194563

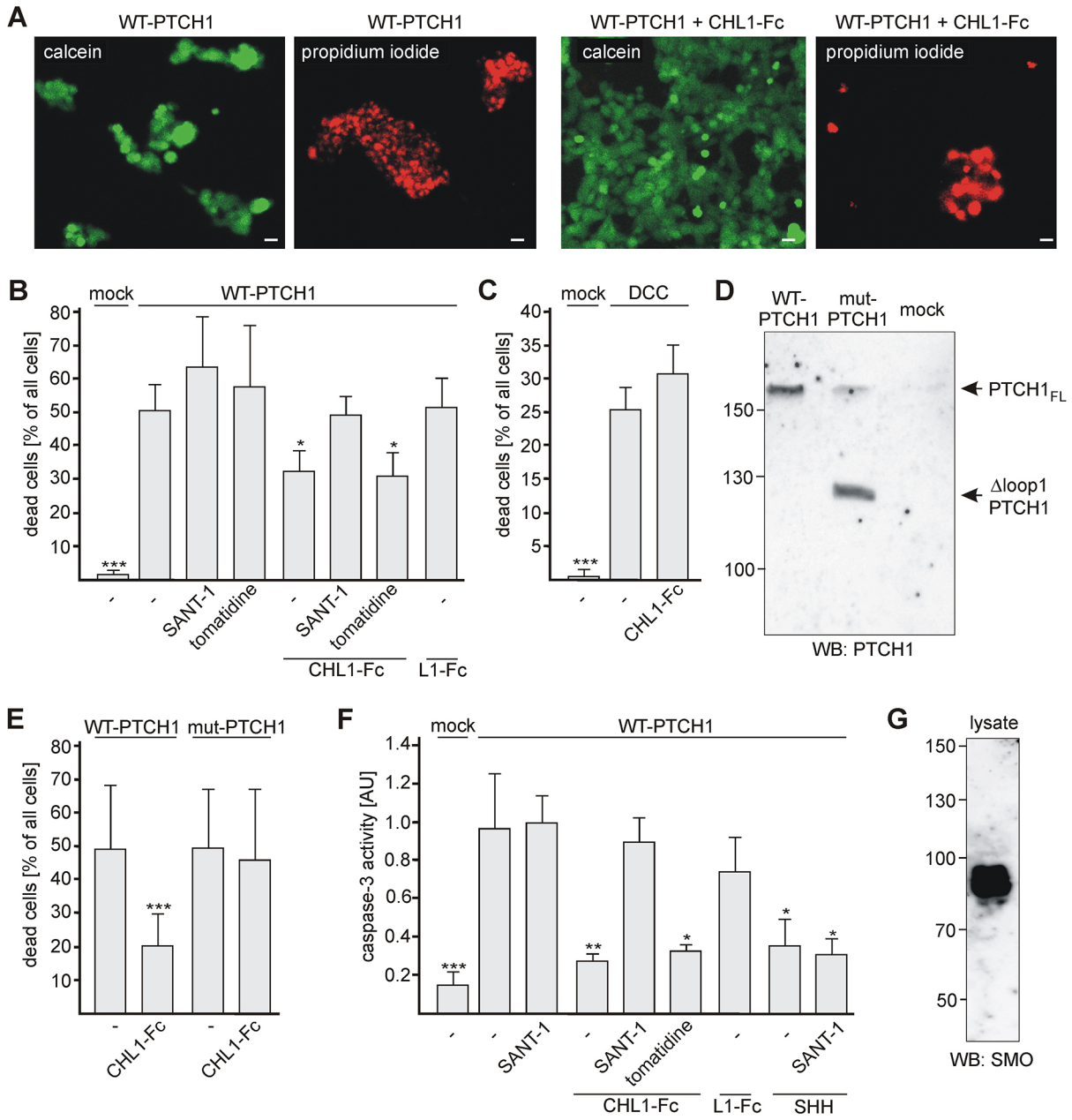

Fig. 4. CHL1–Fc inhibits PTCH1-induced apoptosis in transfected HEK293 cells. HEK293 cells were mock-transfected (B–D,F) or transfected with non-mutated PTCH1 (WT-PTCH1) (A,B,D–F), DCC (C) or with PTCH1 lacking the first extracellular loop (mut-PTCH1) (D,E) followed by cell surface biotinylation (D) or incubation without or with CHL1–Fc, L1–Fc, SHH in the absence (–) or presence of SANT-1 or tomatidine (B,F). (A) Representative images are shown for calcein-positive live (green) and propidium iodide-positive dead (red) cells after transfection with PTCH1 and treatment without or with CHL1–Fc. Scale bars: 20 µm. (D) Cells were subjected to isolation and western blot analysis of biotinylated proteins. Full-length ($PTCH1_{FL}$) and truncated (Δloop1 PTCH1) recognized by the anti-PTCH1 antibody are depicted by arrows. (B,C,E,F) Mean+s.d. values from three independent experiments with three, three and four cell culture wells per treatment and experiment (n=10) (B), with three cell culture wells per treatment and experiment (n=9) (C,F) or with seven, seven and eight cell culture wells per treatment and experiment (n=22) (E) are shown for cell death (B,C,E) or for caspase-3 activity (F). Values were compared to control values obtained for untreated PTCH1-transfected cells (AU, arbitrary units) by using a Kruskal–Wallis test with post-hoc Dunn's multiple comparison test (B,C,E,F) and differences relative to the control group are indicated (*P<0.05; **P<0.001; ***P<0.005). (G) A western blot of HEK293 cell lysate (30 µg protein) with anti-SMO antibody is shown.

therefore hypothesized that ablation of CHL1 leads to enhanced PTCH1-induced apoptosis during the second postnatal week, leading to a loss of these cells. To investigate this question, cerebellar organotypic cultures from 7-day-old mice were subjected, after 5 days in culture, to serum-deprivation for 2 days in the absence or presence of CHL1–Fc, L1–Fc, SANT-1 or tomatidine. Compared to the numbers of dead cells in the absence of CHL1, numbers of dead cells were reduced by CHL1–Fc but unaffected by L1–Fc (Fig. 6A,B). SANT-1, but not tomatidine, inhibited the anti-apoptotic effect of CHL1, but did not influence cell death in the absence of CHL1 (Fig. 6A,B), indicating that binding of CHL1 to PTCH1 prevents PTCH1-induced cell death in a SMO-dependent manner.

To further analyze the effect of CHL1–Fc on apoptosis and caspase-3 activity in cerebellar granule cells, organotypic cultures of

Journal of Cell Science (2017) 130, 2606-2619 doi:10.1242/jcs.194563

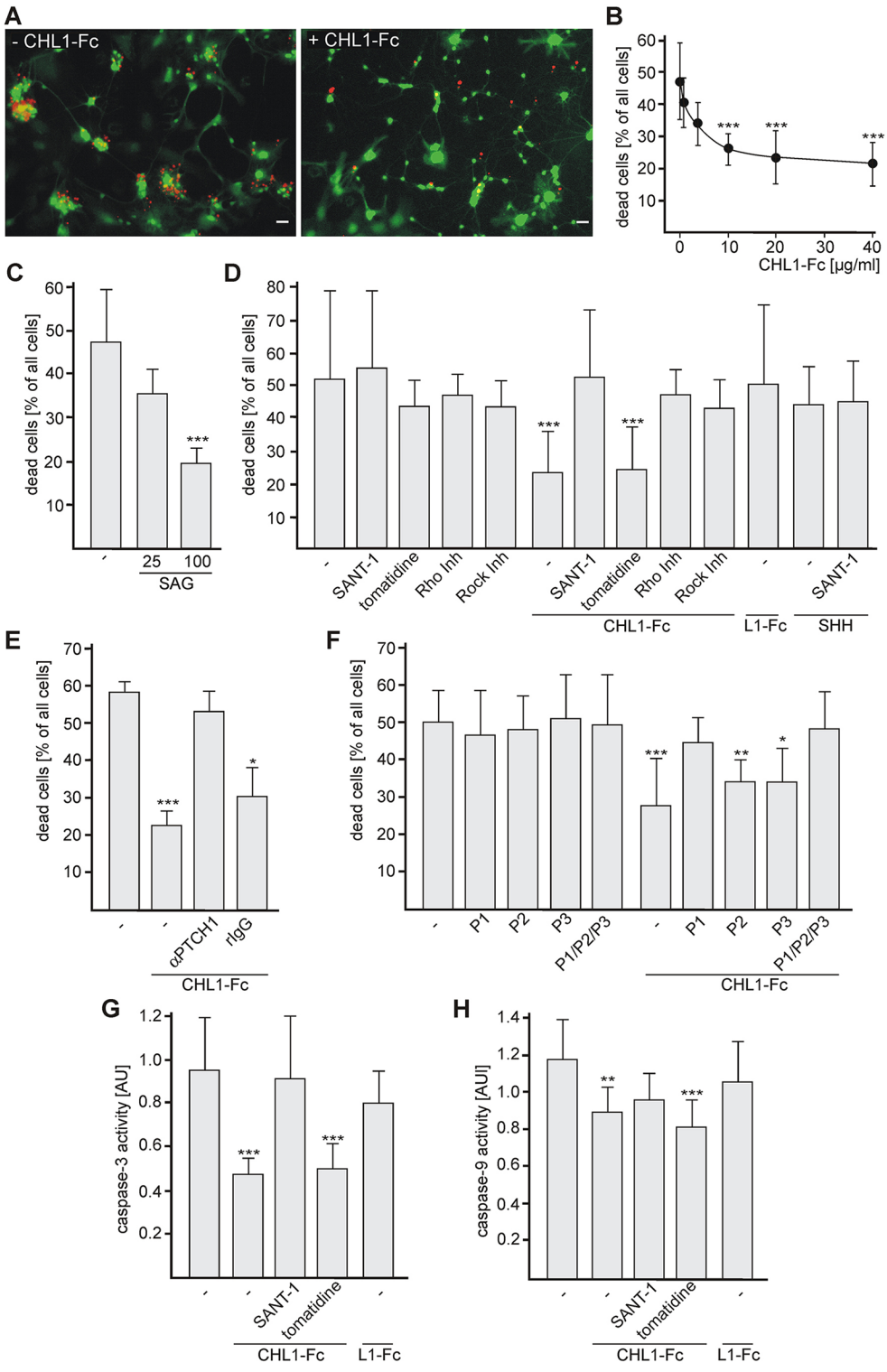

Fig. 5. CHL1–Fc inhibits PTCH1-induced apoptosis in cultures of dissociated cerebellar granule cells and organotypic cerebellar slices via Smo-, RhoA- and ROCK-dependent pathways. Cultures of dissociated neurons from 7-day-old CHL1-deficient mice were maintained for 5 days in serum-containing medium and then subjected to serum-deprivation for 2 days in the absence (–) or presence of CHL1–Fc, L1–Fc, SHH, SAG, SANT-1, tomatidine, RhoA inhibitor (Rho Inh), ROCK inhibitor (Rock Inh) or CHL1-derived peptides CHL1-P1, -P2 and/or -P3, a rat anti-PTCH1 antibody (αPTCH1) or non-immune control antibody (rIgG). (A) Representative images for calcein-positive live (green) and propidium iodide-positive dead (red) cells are shown. Scale bars: 20 µm. (B–H) Mean+s.d. values from three independent experiments with three cell culture wells per treatment and experiment (n=9) (B,C), six independent experiments with three cell culture wells per treatment and experiment (n=18) (D), from four independent experiments with three cell culture wells per treatment and experiment (n=12) (E) or from three independent experiments comprising three, three and four cell culture wells per treatment and experiment (n=10) (F) or with the cell culture wells per treatment and experiment (n=9) (G,H) are shown for cell death (B–F) and for caspase-3 (G) or -9 (H) activities (AU, arbitrary units), respectively. Values were compared to values obtained for samples without additives using Kruskal–Wallis test with post-hoc Dunn's multiple comparison test, and differences relative to the control group are indicated (*P<0.05; **P<0.01; ***P<0.005).

CHL1-deficient cerebellum were subjected to immunostaining for NeuN (also known as RBFOX3), a marker for differentiated granule neurons, and to TdT-mediated dUTP-biotin nick-end labeling (TUNEL) assay or to immunostaining of active caspase-3. Since Purkinje cell loss was also observed in the cerebellum of CHL1-deficient mice (Jakovcevski et al., 2009), cell death and caspase-3 activity in Purkinje cells was determined using an antibody against calbindin, a marker for Purkinje cells. The numbers of cells stained by TUNEL and anti-NeuN antibody or co-stained for NeuN and active caspase were reduced by CHL1–Fc, but not by L1–Fc (Fig. 6C–F). Application of SANT-1 and CHL1–Fc resulted in similar numbers of TUNEL and NeuN double-positive, and active caspase-3 and NeuN double-positive cells, when compared to those without CHL1–Fc or in the presence of only SANT-1 (Fig. 6C,E,F). Cell numbers positive for TUNEL and calbindin, or positive for calbindin and active caspase-3 were reduced by CHL1–Fc, but not by L1–Fc, SANT-1 or by combined SANT-1 and CHL1–Fc application (Fig. 6G,H). These results suggest that binding of CHL1 to PTCH1 inhibits caspase-3-

Journal of Cell Science (2017) 130, 2606-2619 doi:10.1242/jcs.194563

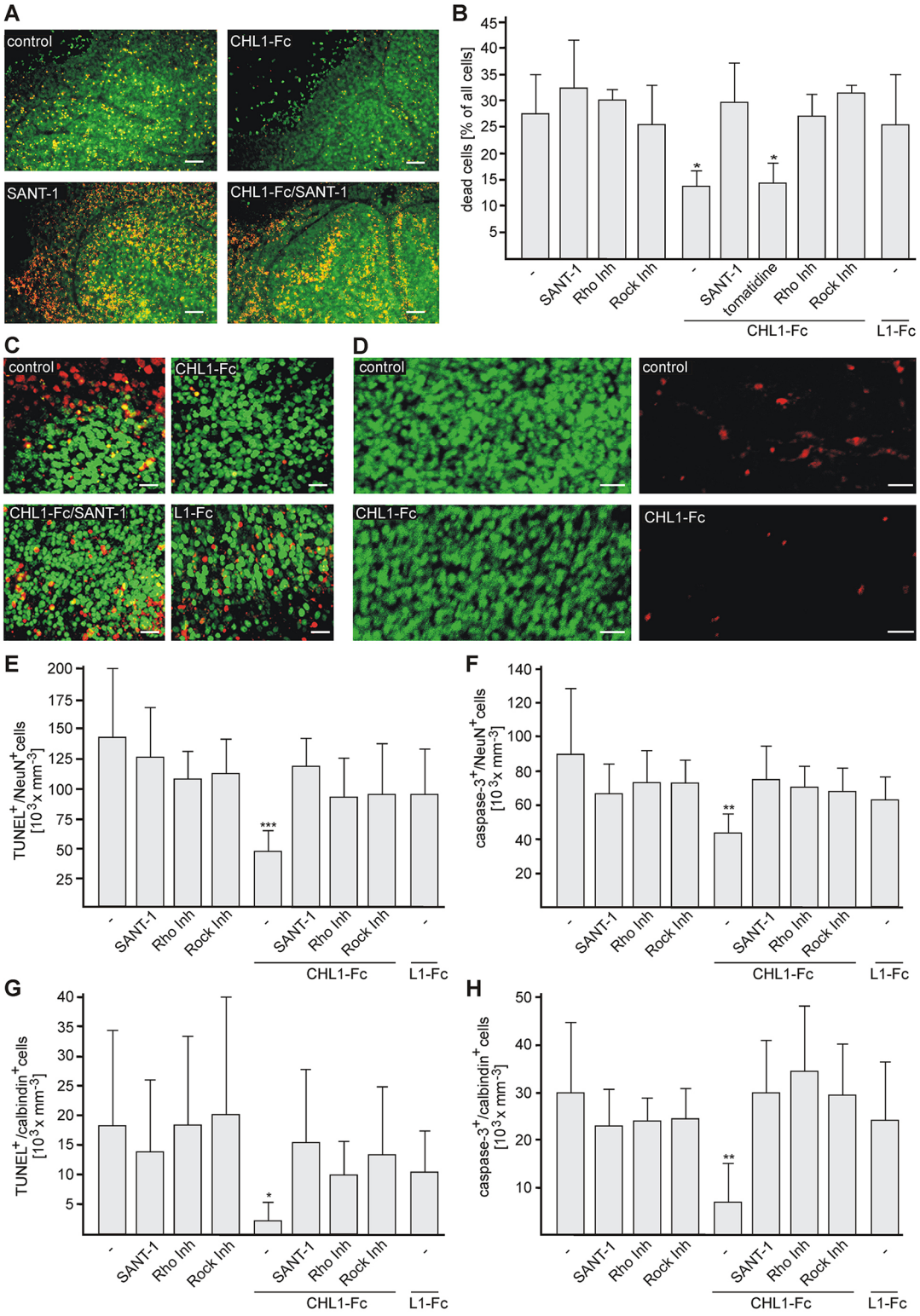

Fig. 6. CHL1–Fc inhibits PTCH1-induced apoptosis of cerebellar granule and Purkinje cells *in vitro*. Organotypic cultures from cerebellum of CHL1-deficient mice were maintained for 5 days in serum-containing medium and then subjected to serum-deprivation for 2 days in the absence or presence of CHL1–Fc, L1–Fc, SANT-1, RhoA inhibitor (Rho Inh) or ROCK inhibitor (Rock Inh). (A) Representative images of slices with calcein-positive live cells (green) and propidium iodide-positive dead cells (red) are shown. Scale bars: 100 µm. (B) Mean+s.d. values from four independent experiments using slices from one animal for all conditions per experiment and two slices per condition and experiment (n=4) are shown for cell death relative to the values without additives (set to 100%). (C,D) Representative images of slices with TUNEL-positive (red) and NeuN-positive (green) cells (C) or with cells positive for NeuN (green) and active caspase-3 (red) (D) are shown. Scale bars: 20 µm. (E–H) Mean+s.d. values from eight independent experiments using slices from one animal for all conditions per experiment and two slices per condition and experiment (n=8) are shown for the number of cells positive for TUNEL and NeuN (E), active caspase-3 and NeuN (F), TUNEL and calbindin (G) or active caspase-3 and calbindin (H) staining. Differences between groups are indicated (*P<0.05; **P<0.01; ***P<0.005; Kruskal–Wallis test with post-hoc Dunn's multiple comparison test).

Journal of Cell Science (2017) 130, 2606-2619 doi:10.1242/jcs.194563

mediated apoptosis of granule and Purkinje cells via SMO-dependent pathways.

CHL1 triggers cellular responses via 'non-canonical' Gli-independent signaling pathways

Binding of hedgehog proteins to PTCH1 triggers cellular responses via 'canonical' Gli-dependent or 'non-canonical' Gli-independent signaling pathways. We therefore investigated whether binding of CHL1 to PTCH1 leads to activation of Gli-dependent canonical signaling pathways. By performing quantitative real-time PCR (qPCR), we determined the transcription levels of PTCH1, Gli-1 and Gli-3, which are known as target genes of PTCH1/SMO activation (Goodrich et al., 1997; Kenney et al., 2003; Pasca di Magliano and Hebrok, 2003; Jacob and Lum, 2007; Robbins et al., 2012; Briscoe and Thérond, 2013). Levels of *Ptch1*, *Gli1* and *Gli3* mRNA from cultures of dissociated cerebellar granule neurons were not altered by application of CHL1–Fc or L1–Fc relative to the mRNA levels in mock-treated cells (Fig. 7A), indicating that CHL1 does not trigger canonical PTCH1 signaling pathways.

Since PTCH1 also mediates hedgehog-triggered non-canonical Gli-independent signaling, such as activation of RhoA via a SMO-dependent pathway (Kasai et al., 2004; Riobo et al., 2006; Lipinski et al., 2008; Jenkins, 2009; Yam et al., 2009; Polizio et al., 2011a,b; Shen et al., 2013), we asked whether CHL1 triggers RhoA activation. In comparison to untreated neurons, application of CHL1–Fc or SAG enhanced the levels of activated RhoA as determined by pulldown assay and ELISA experiments (Fig. 7B–D). In the presence of both SANT-1 and CHL1–Fc, activated RhoA levels declined to those observed in untreated neurons (Fig. 7B–D). The levels of activated RhoA were not altered by SANT-1 alone (Fig. 7B–D). All treatments did not alter the levels of total RhoA (Fig. 7B). These results indicate that activation of SMO by SAG or CHL1–Fc leads to RhoA activation.

To examine whether prevention of PTCH1-induced cell death by CHL1 depends on RhoA activation, cell death was measured in cultures of dissociated CHL1-deficient cerebellar granule cells and organotypic cerebellar slices in the absence or presence of CHL1–Fc and of a RhoA inhibitor. In parallel, an inhibitor against ROCK1 and ROCK2 was probed for its ability to block CHL1-induced cell survival, knowing that ROCK proteins are activated by Rho GTPases and cleavage by caspases (Street and Bryan, 2011). In the absence of CHL1, cell death was unaffected in cultures of dissociated CHL1-deficient neurons and organotypic slices by either inhibitor, but CHL1-induced reduction of cell death was abolished by both inhibitors (Figs 5D and 6B). Both inhibitors also abrogated the influence of CHL1–Fc apoptosis as determined by the TUNEL assay and staining of active caspase-3 in NeuN-positive granule neurons and calbindin-positive Purkinje cells in organotypic cerebellar slices (Fig. 6E–H).

These results suggest that binding of CHL1 to PTCH1 inhibits caspase-3 activity and triggers non-canonical Gli-independent SMO-dependent signal cascades, which activate RhoA and ROCK proteins and trigger responses, such as cell survival.

Ablation of CHL1 leads to enhanced death of granule cells *in vivo* during the second postnatal week

Since CHL1 deficiency results in a loss of cerebellar granule cells in 2-month-old, but not 1-week-old, mice (Jakovcevski et al., 2009),

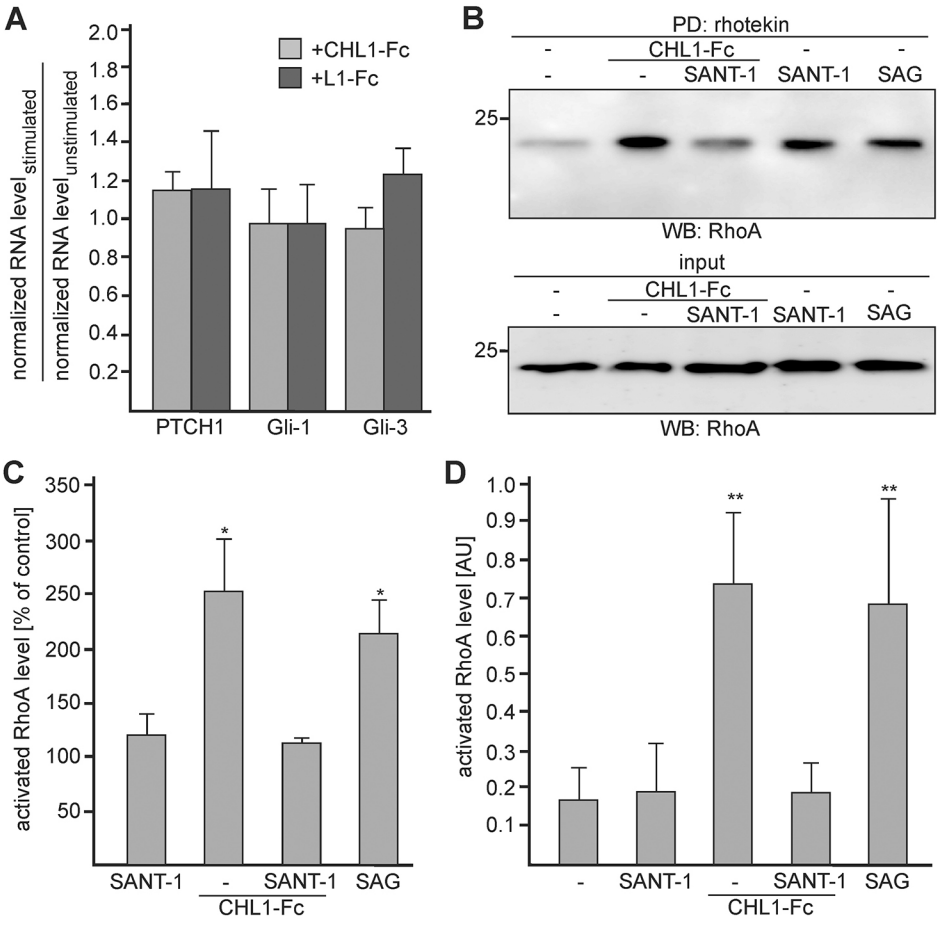

Fig. 7. CHL1 triggers RhoA activation, but does not induce gene expression via SMO activation. Cultures of dissociated cerebellar granule cells from cerebella of 7-day-old CHL1-deficient mice were maintained for 5 (A) or 6 (B-D) days in serum-containing medium and then incubated with CHL1–Fc or L1–Fc for 2 days in serum-free medium (A) or were serum-deprived for 1 day and then treated for 20 min with SAG or SANT-1 alone or with CHL1–Fc in the absence or presence of SANT-1 (B–D). Neurons were subjected to qPCR using PTCH1-, Gli-1-, or Gli-3-specific primers (A), to a pulldown assay followed by western blot analysis with anti-RhoA antibody to determine the level of activated RhoA (B,C), to western blot analysis of cell lysates using the anti-RhoA antibody to determine levels of total RhoA (B) and to an ELISA to quantify levels of activated RhoA (D). (A) Mean+s.d. values from seven independent experiments are shown for *Ptch1*, *Gli1* and *Gli3* mRNA levels in neurons treated with CHL1–Fc or L1–Fc relative to the levels in non-treated neurons. (B) Representative western blots of activated and total RhoA are shown. (C) Mean+s.d. values from four independent pulldown experiments are shown for the activated RhoA levels relative to the values without additives (set to 100%). (D) Mean+s.d. values from three independent ELISA experiments with two cell culture wells per experiment (n=6) are shown for levels of activated RhoA. In C and D, differences relative to the control group are indicated (*P<0.05, **P<0.01; Kruskal–Wallis test with post-hoc Dunn's multiple comparison test).

Journal of Cell Science (2017) 130, 2606-2619 doi:10.1242/jcs.194563

and since the results of the *in vitro* experiments with cultures of dissociated cerebellar granule cells and organotypic slices showed that absence of CHL1 leads to PTCH1-mediated apoptosis and loss of granule cells during the second postnatal week, we investigated whether CHL1-deficient granule cells start to die *in vivo* during the second postnatal week. To this aim, cerebellar slices from 10- and 14-day-old wild-type and CHL1-deficient mice were subjected to staining with antibodies against active caspase-3 and NeuN or calbindin, or to TUNEL assay and NeuN or calbindin immunostaining. Numbers of active caspase-3 and NeuN double-immunopositive neurons were similar in the external cerebellar granule cell layer of 10-day-old CHL1-deficient and wild-type mice, but were increased in the internal granule layer of 10- and 14-day-old CHL1-deficient versus wild-type mice (Fig. 8A,C). The numbers of active caspase-3 and calbindin double-positive apoptotic Purkinje cells were similar in 10- and 14-day-old CHL1-deficient and wild-type mice (Fig. 8D). The numbers of TUNEL and NeuN double-positive neurons were similar in the external granule cell layer of 10- and 14-day-old mice of both genotypes, but were increased in the internal granule cell layer of 10- and 14-day-old CHL1-deficient versus wild-type mice (Fig. 8B, E). No active caspase-3 and NeuN, or TUNEL and calbindin double-positive neurons were detectable in the external granule or Purkinje cell layers, respectively, of 14-day-old CHL1-deficient and wild-type mice (data not shown). These results indicate that CHL1-deficiency *in vivo* leads to apoptosis of granule, but not Purkinje cells, during the second postnatal week.

DISCUSSION

In the present study, we identified CHL1 as a novel, non-canonical ligand of PTCH1. By performing ELISA experiments, we showed that murine CHL1 binds to a sequence stretch in the first extracellular loop of PTCH1 via amino acids 1007–1027 and/or 1050–1070 in its membrane-proximal FNIII domains. Interestingly, cell culture experiments suggested that CHL1 amino acids 1007–1027 mediate its binding to PTCH1. This CHL1 sequence stretch shows similarity to amino acids 51–72 of murine SHH, which binds to PTCH1 via its N-terminal sequences. The murine CHL1 sequence stretch 1007–1027 and the murine SHH sequence stretch 51–72 as well as CHL1 and SHH sequences from other species contain the common motif TLGxxxK/RxxxKIT/S, suggesting that this motif is important for the binding of CHL1 and SHH to their receptor PTCH1. We now show

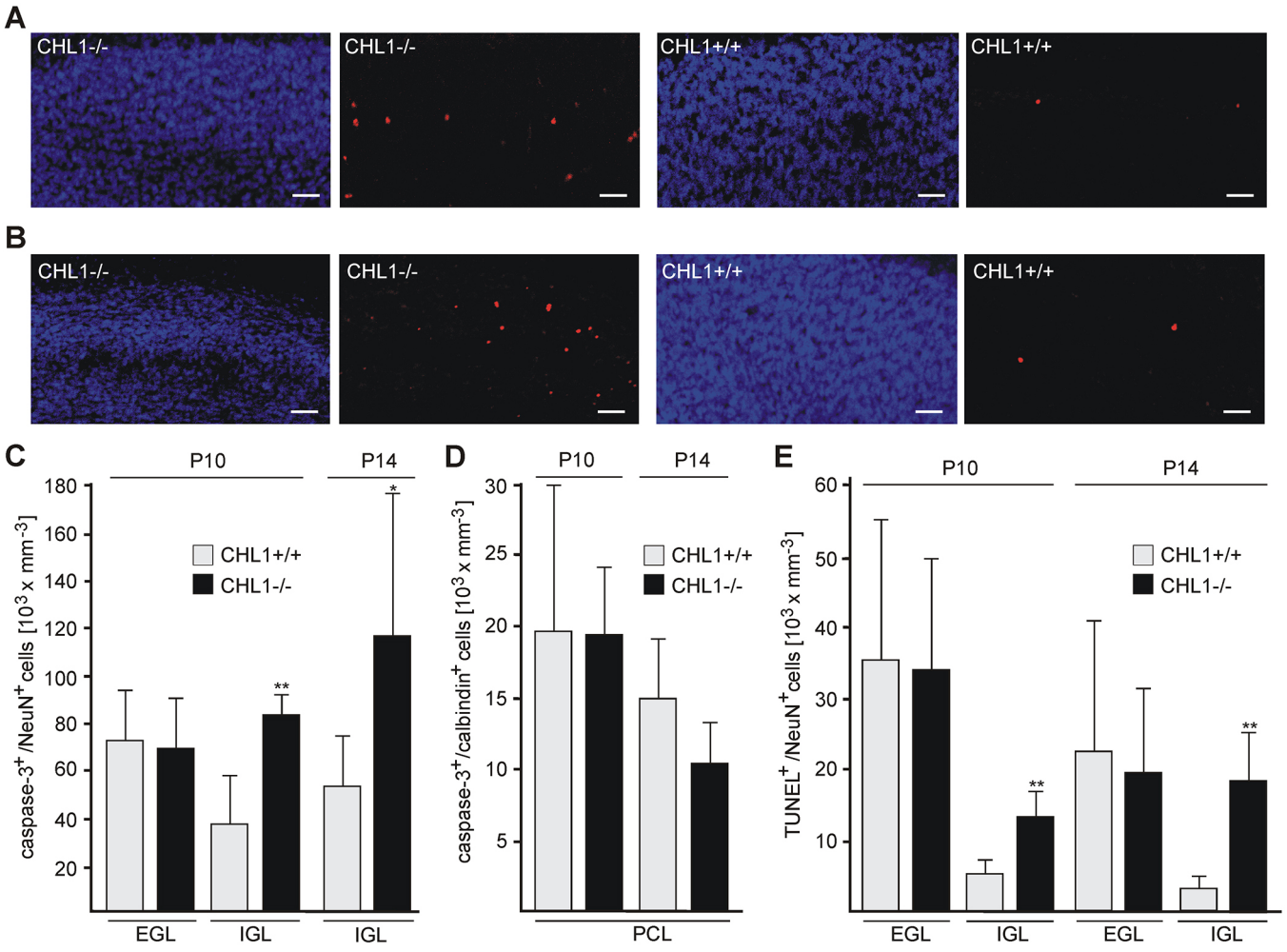

Fig. 8. CHL1–Fc inhibits apoptosis of cerebellar granule cells at early stages of development *in vivo*. Sections of cerebella from 10- or 14-day-old (P10, P14) wild-type (CHL1 +/+) and CHL1-deficient (CHL1 –/–) mice (n=6 animals per group) were stained for active caspase-3 and NeuN or calbindin, or for TUNEL and NeuN. Representative images of DAPI-stained slices with cells positive for TUNEL (red) (A) or active caspase 3 (red) (B) staining are shown. Scale bars: 30 µm. (C–E) Mean+s.d. values are shown for the number of cells positive for active caspase-3 and NeuN (C), for active caspase-3 and calbindin (D) or for TUNEL and NeuN (E) per area in the external granular layer (EGL), internal granular layer (IGL) or Purkinje cell layer (PCL). Differences between groups (*P<0.05, **P<0.01; two-tailed Mann–Whitney U-test) are indicated.

Journal of Cell Science (2017) 130, 2606-2619 doi:10.1242/jcs.194563

that the newly discovered PTCH1 ligand CHL1 activates SMO-dependent signaling pathways and represses caspase-3 and caspase-9 to promote neuronal cell survival. CHL1 does not trigger Gli-dependent transcription, but activates RhoA in a SMO-dependent manner, indicating that CHL1 stimulates non-canonical rather than canonical hedgehog signaling pathways. The CHL1-induced activation of non-canonical hedgehog signal transduction pathways via RhoA and ROCK proteins promotes the cell survival of postmitotic cerebellar granule cells during the crucial morphogenetic stages of postnatal cerebellar development. Interestingly, SHH does not promote survival of CHL1-deficient cerebellar granule cells in the cell death assay, suggesting that SHH and CHL1 trigger different signaling pathways and that the SHH-triggered signal pathways cannot be activated or are not active in differentiated post-migratory granule cells in the second postnatal week. The notion that SHH and CHL1 trigger different signaling pathways is supported by the finding that SHH-induced survival of PTCH1-overexpressing HEK293 cells is not blocked by the SMO antagonist SANT-1 in contrast to CHL1–Fc-induced survival, which is inhibited by SANT-1. This result suggests that SHH triggers SMO-independent pathways in a certain cellular context, whereas CHL1 triggers SMO-dependent pathways. Furthermore, CHL1 inhibits and SHH promotes differentiation and proliferation of neural progenitor cells and of granule cell precursors (Pons et al., 2001; Jakovcevski et al., 2009; Huang et al., 2011; Komada, 2012; Álvarez-Buylla and Ihrie, 2014; Katic et al., 2014), suggesting that the opposite CHL1- and SHH-induced cellular responses during early postnatal development are mediated through different signaling pathways.

Absence of CHL1 may lead to enhanced proliferation and differentiation of granule cells via SHH, resulting in deficient innervation of stellate and Purkinje cells, aberrant branching and orientation of stellate cell axons and aberrant arborizations of Purkinje cell dendrites (Ango et al., 2008; Jakovcevski et al., 2009). Defective innervation of Purkinje cell dendrites by granule cell axons in CHL1-deficient mice would be likely to cause loss of Purkinje cells. Notably, increased apoptosis of Purkinje cells was observed in organotypic cerebellar cultures from CHL1-deficient mice upon serum deprivation, and this enhanced apoptosis was reduced by CHL1–Fc in a SMO-dependent manner, suggesting that binding of CHL1 to PTCH1 regulates apoptosis of Purkinje cells. Given that the final numbers of Purkinje cells are regulated by apoptosis already during the first postnatal week (Ghoumari et al., 2000), no enhanced apoptosis of Purkinje cells was found in histological sections from 10- or 14-day-old CHL1-deficient mice.

In a previous study, we observed that CHL1 delays differentiation of granule cell precursors and that ablation of CHL1 causes precocious differentiation of granule cell precursors and migration of these premature cells into the internal granular layer (Katic et al., 2014). These observations led to the hypothesis that these prematurely differentiated post-migratory neurons are eliminated by apoptosis after their migration into the internal granule layer, resulting in a loss of granule cells in the internal granule layer of 2-month-old CHL1-deficient mice (Jakovcevski et al., 2009). Here, we provide evidence that enhanced apoptosis of post-migratory neurons takes place in the internal granule layer of CHL1-deficient mice during the second postnatal week. Since CHL1 is expressed by cerebellar granule cells (Jakovcevski et al., 2009) and can be released as a soluble extracellular fragment upon proteolytic cleavage (Naus et al., 2004), it is conceivable that soluble CHL1 fragments and/or cell surface-bound CHL1 bind to PTCH1 in a *trans*-position and thereby inhibit PTCH1-induced cell death of post-migratory cerebellar granule cells in the internal granule layer.

Since apoptosis of cerebellar granule cells is abnormal in CHL1-deficient mice during the second postnatal week and since CHL1–Fc rescues these defects *in vitro* via a PTCH1- and SMO-dependent pathway, we propose that PTCH1/SMO-dependent apoptosis of granule cells during later developmental stages is predominantly regulated by CHL1, with SHH playing a minor role at this time. This idea is supported by the observation that SHH does not promote cell survival of cultured cerebellar granule cells upon serum deprivation.

The combined observations from the present study indicate that a finely balanced functional interplay of CHL1 with PTCH1 and SMO triggers neuronal survival during postnatal cerebellar development.

MATERIALS AND METHODS

Animals

CHL1-deficient mice (Montag-Sallaz et al., 2002), which had been back-crossed onto the C57BL/6J background for more than eight generations, and age-matched wild-type littermates of either sex were used. All animal experiments were approved by the authorities of the State of Hamburg (permit numbers ORG 535 and G09/098).

Antibodies and reagents

Rabbit antibodies against the extracellular domain of CHL1, L1 or NCAM were prepared as described previously (Chen et al., 1999; Rolf et al., 2003). Goat anti-CHL1 antibody (AF2147; lot, VEX0113121), rat anti-PTCH1 antibody (MAB41051; lot, ZKA0214101), rat anti-SHH antibody (MAB4641; lot, HAO0309091) and rabbit antibody against active caspase-3 (AF835; lot, CFZ3414111) were from R&D Systems. Rat L1 antibody 555 and NCAM antibody P61 have been described previously (Makhina et al., 2009; Cassens et al., 2010). Rabbit anti-PTCH1 antibody (17520-1-AP; lot, not specified), anti-SMO antibody (TA318627; lot, 52042) and rabbit anti-SHH antibody (20697-1-AP; lot, not specified) were from Acris. Mouse anti-calbindin-D-28K antibody (C9848; lot, 063M4760) was from Sigma-Aldrich and mouse anti-NeuN antibody (MAB377; lot, LV1427917) was from Merck-Millipore. Preparation of CHL1–Fc, L1–Fc, and NCAM-Fc has been described previously (Chen et al., 1999). Horseradish peroxidase (HRP)-coupled and fluorescent dye-coupled secondary antibodies and human Fc were from Dianova. SANT-1 {N-[(3,5-dimethyl-1-phenyl-1H-pyrazol-4-yl) methylene]-4-(phenylmethyl)-1-piperazinamine; CAS 304909-07-7} and tomatidine (3β-hydroxy-5α-tomatidine hydrochloride; CAS 6192-62-7) were from Merck-Millipore. SAG {3-chloro-N-[trans-4-(methylamino)cyclohexyl]-N-[[3-(4-pyridinyl) phenyl]methyl]-benzo[b]thiophene-2-carboxamide; CAS 912545-86-9} and recombinant patched-1 protein (MBS2011579) were from Biozol. PTCH1 and DCC expression vectors were from Patrick Mehlen (CNRS, Lyon, France) and Rob Meijers (EMBL, Hamburg, Germany), respectively. The CHL1-derived peptides P1 (KTKSLLDGRTHPKEVNILRFSGQR), P2 (EEGATLGEGSKGIRKITEGVN), P3 (TKNWGDNDSIFQDVIETR-GRE) and the L1-derived peptide PL1 (ELEDITIFNSSTVLVRWRPVD) were from Schafer-N (Copenhagen, Denmark). Rho inhibitor II, Y16 (#5040430001) and the ROCK inhibitor Y-27632 (#10-2301) were from Merck-Millipore and TEBU, respectively. The recombinant N-terminal fragment of rat SHH was from R&D Systems. The N-terminal fragment of human SHH was provided by Elisa Martí (Instituto de Biología Molecular de Barcelona, Barcelona, Spain) (Pons and Martí, 2000; Pons et al., 2001).

Phage display

The Ph.D.-12™ Phage Display Peptide Library (New England Biolabs) was used as described previously (Wang et al., 2011).

Sequence analysis

The phage peptide sequences were subjected to online database searches using protein–protein BLAST® (http://blast.ncbi.nlm.nih.gov/Blast.cgi) and UniProtKB/Swiss-Prot databases with filter settings for 'Organism' and 'Entrez Query' being 'Mus musculus (taxid:10090)' and 'transmembrane AND receptor AND death', 'transmembrane AND receptor AND neural',

Journal of Cell Science (2017) 130, 2606-2619 doi:10.1242/jcs.194563

'transmembrane AND receptor AND development', 'receptor AND plasma membrane' or 'signaling AND plasma membrane'. Hit sequences, were inspected for highly and weakly conserved residues to create sequence motifs that were applied to online screening using the ScanProsite tool of ExPASy Bioinformatics Resource Portal (http://prosite.expasy.org/scanprosite/) with filter settings 'mammalia' or 'vertebrate' for taxonomy to identify similarities in other species.

To identify sequence similarities between SHH and CHL1, sequence stretches of mouse SHH and CHL1 were applied to the online SIM-Alignment Tool for Protein Sequences of the ExPASy Bioinformatics Resource Portal (http://web.expasy.org/sim/). Sequence stretches showing sound similarities were used to create sequence motifs which were applied to the ScanProsite tool to identify similarities in other species and other hedgehog proteins.

Cloning of the PTCH1 deletion mutant, transfection of HEK293 cells and treatment of transfected cells

The PTCH1-expressing vector served as template for cloning the PTCH1 deletion mutant using the Q5® Site-Directed Mutagenesis Kit (New England Biolabs) and the primers 5′-GTCAGTGTCATCCGAGTG-3′ and 5′-GAGATTAGCTGCCTTTAATC-3′. HEK293 cells (ATCC CRL-1573™; tested for contamination every 3 months) were plated in 6-well plates (Nunc) at a density of 2×10^5 cells/well and maintained in DMEM supplemented with 0.580 mg/ml L-glutamine, 4.5 mg/ml glucose, 10% fetal calf serum, and 100 µg/ml penicillin-streptomycin. At 70–80% confluence, cells were washed with HBSS and transfected with PTCH1 or DCC by using Lipofectamine® LTX Reagent with PLUS™ Reagent (Invitrogen) and 2 µg/ml plasmid DNA. The medium was changed 6 h thereafter, and cells were treated with 20 µg/ml CHL1–Fc or L1–Fc, 6 µg/ml SHH and/or 120 nM SANT-1 or tomatidine for 24 h before cell death was analyzed.

qPCR

qPCR was performed as described previously (Westphal et al., 2016).

Immunoprecipitation, RhoA activation assay, cell surface biotinylation and western blot analysis

Immunoprecipitation, western blot analysis and densitometry as well as cell surface biotinylation of HEK293 cells 24 h after transfection was performed as described previously (Makhina et al., 2009; Westphal et al., 2016). Rabbit anti-CHL1, L1 or NCAM antibody (10 µl serum) or rabbit anti-PTCH1 antibody (5 µg IgG) were used for immunoprecipitation. Rat anti-PTCH1 antibody (1:100), goat anti-CHL1 antibody (1:1000), rat anti-L1 antibody 555 (1:2000) or rat anti-NCAM antibody P61 (1:1000) and HRP-conjugated secondary antibodies (1:20,000) were used for western blot analysis of the immunoprecipitates, and rabbit anti-PTCH1 antibody (1:1000) and a HRP-conjugated secondary antibody (1:20,000) was used for western blot analysis of biotinylated proteins. For determination of the level of activated RhoA, the pulldown RhoA activation assay Biochem Kit (#BK036-S; Cytoskeleton, Denver, CO, USA) and the G-LISA® RhoA activation assay Biochem Kit (#BK124; Cytoskeleton) with duplicates per sample were used.

ELISA and label-free binding assay

ELISA was performed as previously described (Makhina et al., 2009; Loers et al., 2012). HRP-conjugated anti-human Fc (1:2000) was used for determination of CHL-Fc, NCAM-Fc or Fc binding and rat SHH antibody (1:100) and HRP-conjugated anti-rat antibody (1:2000) were used for detection of SHH binding. In competition ELISA, competitors were pre-incubated for 30 min.

Label-free binding assay was performed as described previously (Loers et al., 2012). CHL1–Fc, NCAM-Fc or Fc were coated and incubated with different amounts of the recombinant PTCH1 fragment. Binding was measured by determination of peak wavelength shift and CHL1–Fc- and NCAM-Fc-specific binding was calculated by subtraction of values from Fc binding.

Preparation of dissociated cerebellar granule cells and cerebellar organotypic slice cultures

Cultures of dissociated cerebellar granule cells were prepared from 6- to 7-day-old mice as described previously (Loers et al., 2012). Organotypic cultures were prepared from 7-day-old mice using a modification of the protocol from Stoppini et al. (1991). Briefly, cerebella were sliced in 300 µm thick sections using a tissue chopper. Slices with intact structure and of similar size representing similar structures for each group from one animal per experiment were randomly chosen and placed on Millicell cell culture inserts (Millipore). Inserts with two slices were placed in six-well plates with pre-warmed incubation medium [75% MEM, 25% horse serum, 25 mM HEPES, 1 mM glutamine, 5 mg/ml D-glucose, 100 U/ml penicillin-streptomycin]. The dissociated neurons and slices were maintained in an incubator at 37°C, 5% CO_2 and 90% humidity with one medium exchange on the third day. After 5 days in culture, the medium was changed to serum-free medium and the samples were incubated for an additional 2 days in the absence or presence of 20 µg/ml CHL1–Fc or L1–Fc, 6 µg/ml SHH, 120 nM SANT-1 or tomatidine or 60 µM Rho or ROCK inhibitor.

Tissue preparation, immunohistochemistry and proximity ligation assay

Preparation of coronal 25-µm-thick cerebellar sections, immunostaining and proximity ligation assay using the Duolink detection reagents RED were performed as described previously (Jakovcevski et al., 2009; Katic et al., 2014). Mixtures of goat anti-CHL1 antibody (1:100) and rat anti-PTCH1 antibody (1:100) and of donkey Cy3-conjugated anti-goat-IgG and Cy2-conjugated anti-rat-IgG antibodies (1:200) were used for the detection of CHL1 and PTCH1. Mixtures of the rabbit antibody against activated caspase-3 (1:1000) and mouse anti-NeuN antibody (1:500) or anti-calbindin antibody (1:1000) and of donkey Cy2-conjugated anti-rabbit-IgG and Cy3-conjugated anti-mouse-IgG antibodies (1:200) were used for the detection of active caspase and NeuN or calbindin. The mouse anti-NeuN antibody (1:500), a donkey Cy2-conjugated anti-mouse-IgG antibody (1:200) and the In Situ Cell Detection Kit, TMR red (Roche; #12156792910) were used for the detection of NeuN-positive apoptotic cells.

For the proximity ligation assay, anti-PTCH1 antibody alone (1:100; control) or mixtures of goat anti-CHL1 (1:100) and rabbit anti-PTCH1 or anti-SHH antibodies (1:100) and Duolink anti-goat PLA probe MINUS and Duolink anti-rabbit PLA probe PLUS were used.

Microphotographs were taken with an Olympus Fluoview FV1000 confocal laser-scanning microscope in sequential mode with a 60× objective and processed using Photoshop CS5 software (Adobe Systems) to adjust brightness and contrast.

Determination of cell death, apoptosis and caspase-3 and -9 activities

If not stated otherwise, cultures of dissociated cerebellar granule cells, organotypic cerebellar slices or mock-transfected or transfected HEK293 cells were serum-deprived for 2 days in the absence or presence of additives as indicated.

Determination of cell death using calcein-AM and propidium iodide was performed as described previously (Loers et al., 2005). Numbers of calcein-positive (live) and propidium iodide-positive (dead) cells were counted in four randomly chosen areas of a microscopic field (10× magnification) per cell culture well and in five images per slice. Cell death was determined as number of dead cells relative to the total numbers of dead and live cells.

For determination of apoptosis in tissue slices, the TUNEL assay or immunostaining of active caspase-3 were performed. Briefly, sections were incubated with TUNEL mixture for 1 h at 37°C, washed with PBS and incubated with blocking solution and with primary and secondary antibodies for 1 h each at room temperature followed by mounting with Roti-Mount FluorCare DAPI (Carl Roth).

For determination of apoptotic cells in organotypic cerebellar cultures, slices were washed once with PBS, fixed with 4% formaldehyde in PBS for 1 h at room temperature, washed once with PBS and incubated in cold 20% methanol in PBS for 5 min. After washing with PBS, slices were subjected to permeabilization with 0.5% Triton X-100 in PBS at 4°C for 2 days followed by incubation with 20% bovine serum albumin (BSA) in PBS overnight at 4°C. The slices were cut off the cell culture inserts and transferred to 48-well plates. Slices were then incubated with TUNEL mixture and primary and secondary antibodies and mounted.

Numbers of apoptotic cells positive in the TUNEL assay or immunostaining for active caspase-3 were quantified by stereological analysis as described previously (Jakovcevski et al., 2009; Katic et al., 2014). Briefly, two cortical fields in the section, one in the most caudal folium and one in the third folium rostral to the first one, were delineated and numbers of cells positive for NeuN or calbindin and activated caspase-3 or TUNEL were counted in three microscopic fields of five sections (25 µm; every ten serial sections).

For determination of caspase-9 and -3 activities, the Caspase-Glo 9 Assay from Promega (G8210) and the Caspase-3 Colorimetric Assay Kit from BioCat (K106-100-BV) were used, and the absorbance or luminescence of the caspase-3 or caspase-9 cleaved substrate, respectively, were measured in duplicates.

Statistical analysis

All data are presented as group mean values. Groups were compared by Kruskal–Wallis test with post-hoc Dunn's multiple comparison test or by two-tailed Mann–Whitney *U*-test using Prism 5.0 software (GraphPad). Statistical tests used for comparisons are indicated in the figure legends.

Acknowledgements

We are grateful to Eva Kronberg for excellent animal care, to Ute Bork for excellent technical assistance, Patrick Mehlen for the PTCH1 expression vector, Rob Meijers for the DCC expression vector, Elisa Martí for recombinant SHH, and Fabio Morellini for performing the statistical analysis.

Competing interests

The authors declare no competing or financial interests.

Author contributions

Conceptualization: M.S., R.K.; Methodology: J.K., G.L., R.K.; Formal analysis: J.K., G.L., R.K.; Investigation: J.K., G.L., J.T., R.K.; Writing - original draft: M.S., R.K.; Writing - review & editing: G.L.; Visualization: J.K.; Supervision: M.S., R.K.; Project administration: G.L.; Funding acquisition: M.S.

Funding

Melitta Schachner is supported by the Li Ka Shing Foundation at Shantou University Medical College. Jelena Katic received a doctoral scholarship from the German Academic Exchange Service (Deutscher Akademischer Austauschdienst, DAAD).

References

Álvarez-Buylla, A. and Ihrie, R. A. (2014). Sonic hedgehog signaling in the postnatal brain. *Semin. Cell. Dev. Biol.* **33**, 105-111.

Ango, F., Wu, C., Van der Want, J. J., Wu, P., Schachner, M. and Huang, Z. J. (2008). Bergmann glia and the recognition molecule CHL1 organize GABAergic axons and direct innervation of Purkinje cell dendrites. *PLoS Biol.* **6**, e103.

Briscoe, J. and Thérond, P. P. (2013). The mechanisms of Hedgehog signalling and its roles in development and disease. *Nat. Rev. Mol. Cell Biol.* **14**, 418-431.

Buhusi, M., Midkiff, B. R., Gates, A. M., Richter, M., Schachner, M. and Maness, P. F. (2003). Close homolog of L1 is an enhancer of integrin-mediated cell migration. *J. Biol. Chem.* **278**, 25024-25031.

Cassens, C., Kleene, R., Xiao, M.-F., Friedrich, C., Dityateva, G., Schafer-Nielsen, C. and Schachner, M. (2010). Binding of the receptor tyrosine kinase TrkB to the neural cell adhesion molecule (NCAM) regulates phosphorylation of NCAM and NCAM-dependent neurite outgrowth. *J. Biol. Chem.* **285**, 28959-28967.

Charron, F. and Tessier-Lavigne, M. (2005). Novel brain wiring functions for classical morphogens: a role as graded positional cues in axon guidance. *Development* **132**, 2251-2262.

Chen, S., Mantei, N., Dong, L. and Schachner, M. (1999). Prevention of neuronal cell death by neural adhesion molecules L1 and CHL1. *J. Neurobiol.* **38**, 428-439.

Chen, J. K., Taipale, J., Young, K. E., Maiti, T. and Beachy, P. A. (2002). Small molecule modulation of Smoothened activity. *Proc. Natl. Acad. Sci. USA* **99**, 14071-14076.

Demyanenko, G. P., Schachner, M., Anton, E., Schmid, R., Feng, G., Sanes, J. and Maness, P. F. (2004). Close homolog of L1 modulates area-specific neuronal positioning and dendrite orientation in the cerebral cortex. *Neuron* **44**, 423-437.

Demyanenko, G. P., Siesser, P. F., Wright, A. G., Brennaman, L. H., Bartsch, U., Schachner, M. and Maness, P. F. (2011). L1 and CHL1 cooperate in thalamocortical axon targeting. *Cereb. Cortex* **21**, 401-412.

Fombonne, J., Bissey, P.-A., Guix, C., Sadoul, R., Thibert, C. and Mehlen, P. (2012). Patched dependence receptor triggers apoptosis through ubiquitination of caspase-9. *Proc. Natl. Acad. Sci. USA* **109**, 10510-10515.

Ghoumari, A. M., Wehrlé, R., Bernard, O., Sotelo, C. and Dusart, I. (2000). Implication of Bcl-2 and Caspase-3 in age-related Purkinje cell death in murine organotypic culture: an in vitro model to study apoptosis. *Eur. J. Neurosci.* **12**, 2935-2949.

Goodrich, L. V., Milenković, L., Higgins, K. M. and Scott, M. P. (1997). Altered neural cell fates and medulloblastoma in mouse patched mutants. *Science* **277**, 1109-1113.

Hillenbrand, R., Molthagen, M., Montag, D. and Schachner, M. (1999). The close homologue of the neural adhesion molecule L1 (CHL1): patterns of expression and promotion of neurite outgrowth by heterophilic interactions. *Eur. J. Neurosci.* **11**, 813-826.

Holm, J., Hillenbrand, R., Steuber, V., Bartsch, U., Moos, M., Lübbert, H., Montag, D. and Schachner, M. (1996). Structural features of a close homologue of L1 (CHL1) in the mouse: a new member of the L1 family of neural recognition molecules. *Eur. J. Neurosci.* **8**, 1613-1629.

Huang, X., Zhu, L.-L., Zhao, T., Wu, L.-Y., Wu, K.-W., Schachner, M., Xiao, Z.-C. and Fan, M. (2011). CHL1 negatively regulates the proliferation and neuronal differentiation of neural progenitor cells through activation of the ERK1/2 MAPK pathway. *Mol. Cell. Neurosci.* **46**, 296-307.

Jacob, L. and Lum, L. (2007). Deconstructing the hedgehog pathway in development and disease. *Science* **318**, 66-68.

Jakovcevski, I., Wu, J., Karl, N., Leshchyns'ka, I., Sytnyk, V., Chen, J., Irintchev, A. and Schachner, M. (2007). Glial scar expression of CHL1, the close homolog of the adhesion molecule L1, limits recovery after spinal cord injury. *J. Neurosci.* **27**, 7222-7233.

Jakovcevski, I., Siering, J., Hargus, G., Karl, N., Hoelters, L., Djogo, N., Yin, S., Zecevic, N., Schachner, M. and Irintchev, A. (2009). Close homologue of adhesion molecule L1 promotes survival of Purkinje and granule cells and granule cell migration during murine cerebellar development. *J. Comp. Neurol.* **513**, 496-510.

Jenkins, D. (2009). Hedgehog signalling: emerging evidence for non-canonical pathways. *Cell. Signal.* **21**, 1023-1034.

Kasai, K., Takahashi, M., Osumi, N., Sinnarajah, S., Takeo, T., Ikeda, H., Kehrl, J. H., Itoh, G. and Arnheiter, H. (2004). The G12 family of heterotrimeric G proteins and Rho GTPase mediate Sonic hedgehog signalling. *Genes Cells* **9**, 49-58.

Katic, J., Loers, G., Kleene, R., Karl, N., Schmidt, C., Buck, F., Zmijewski, J. W., Jakovcevski, I., Preissner, K. T. and Schachner, M. (2014). Interaction of the cell adhesion molecule CHL1 with vitronectin, integrins, and the plasminogen activator inhibitor-2 promotes CHL1-induced neurite outgrowth and neuronal migration. *J. Neurosci.* **34**, 14606-14623.

Kenney, A. M., Cole, M. D. and Rowitch, D. H. (2003). Nmyc upregulation by sonic hedgehog signaling promotes proliferation in developing cerebellar granule neuron precursors. *Development* **130**, 15-28.

Komada, M. (2012). Sonic hedgehog signaling coordinates the proliferation and differentiation of neural stem/progenitor cells by regulating cell cycle kinetics during development of the neocortex. *Congenit. Anom. (Kyoto)* **52**, 72-77.

Lipinski, R. J., Bijlsma, M. F., Gipp, J. J., Podhaizer, D. J. and Bushman, W. (2008). Establishment and characterization of immortalized Gli-null mouse embryonic fibroblast cell lines. *BMC Cell Biol.* **9**, 49.

Loers, G., Chen, S., Grumet, M. and Schachner, M. (2005). Signal transduction pathways implicated in neural recognition molecule L1 triggered neuroprotection and neuritogenesis. *J. Neurochem.* **92**, 1463-1476.

Loers, G., Makhina, T., Bork, U., Dörner, A., Schachner, M. and Kleene, R. (2012). The interaction between cell adhesion molecule L1, matrix metalloproteinase 14, and adenine nucleotide translocator at the plasma membrane regulates L1-mediated neurite outgrowth of murine cerebellar neurons. *J. Neurosci.* **32**, 3917-3930.

Makhina, T., Loers, G., Schulze, C., Ueberle, B., Schachner, M. and Kleene, R. (2009). Extracellular GAPDH binds to L1 and enhances neurite outgrowth. *Mol. Cell. Neurosci.* **41**, 206-218.

Maness, P. F. and Schachner, M. (2007). Neural recognition molecules of the immunoglobulin superfamily: signaling transducers of axon guidance and neuronal migration. *Nat. Neurosci.* **10**, 19-26.

Mehlen, P., Rabizadeh, S., Snipas, S. J., Assa-Munt, N., Salvesen, G. S. and Bredesen, D. E. (1998). The DCC gene product induces apoptosis by a mechanism requiring receptor proteolysis. *Nature* **395**, 801-804.

Mille, F., Thibert, C., Fombonne, J., Rama, N., Guix, C., Hayashi, H., Corset, V., Reed, J. C. and Mehlen, P. (2009). The Patched dependence receptor triggers apoptosis through a DRAL-caspase-9 complex. *Nat. Cell Biol.* **11**, 739-746.

Montag-Sallaz, M., Schachner, M. and Montag, D. (2002). Misguided axonal projections, neural cell adhesion molecule 180 mRNA upregulation, and altered behavior in mice deficient for the close homolog of L1. *Mol. Cell. Biol.* **22**, 7967-7981.

Naus, S., Richter, M., Wildeboer, D., Moss, M., Schachner, M. and Bartsch, J. W. (2004). Ectodomain shedding of the neural recognition molecule CHL1 by the metalloprotease-disintegrin ADAM8 promotes neurite outgrowth and suppresses neuronal cell death. *J. Biol. Chem.* **279**, 16083-16090.

Nikonenko, A. G., Sun, M., Lepsveridze, E., Apostolova, I., Petrova, I., Irintchev, A., Dityatev, A. and Schachner, M. (2006). Enhanced perisomatic inhibition and

impaired long-term potentiation in the CA1 region of juvenile CHL1-deficient mice. *Eur. J. Neurosci.* **23**, 1839-1852.

Pasca di Magliano, M. and Hebrok, M. (2003). Hedgehog signalling in cancer formation and maintenance. *Nat. Rev. Cancer* **3**, 903-911.

Polizio, A. H., Chinchilla, P., Chen, X., Kim, S., Manning, D. R. and Riobo, N. A. (2011a). Heterotrimeric Gi proteins link Hedgehog signaling to activation of Rho small GTPases to promote fibroblast migration. *J. Biol. Chem.* **286**, 19589-19596.

Polizio, A. H., Chinchilla, P., Chen, X., Manning, D. R. and Riobo, N. A. (2011b). Sonic Hedgehog activates the GTPases Rac1 and RhoA in a Gli-independent manner through coupling of smoothened to Gi proteins. *Sci. Signal.* **4**, pt7.

Pons, S. and Martí, E. (2000). Sonic hedgehog synergizes with the extracellular matrix protein vitronectin to induce spinal motor neuron differentiation. *Development* **127**, 333-342.

Pons, S., Trejo, J. L., Martínez-Morales, J. R. and Martí, E. (2001). Vitronectin regulates Sonic hedgehog activity during cerebellum development through CREB phosphorylation. *Development* **128**, 1481-1492.

Riobo, N. A., Saucy, B., Dilizio, C. and Manning, D. R. (2006). Activation of heterotrimeric G proteins by Smoothened. *Proc. Natl. Acad. Sci. USA* **103**, 12607-12612.

Robbins, D. J., Fei, D. L. and Riobo, N. A. (2012). The Hedgehog signal transduction network. *Sci. Signal.* **5**, re6.

Rolf, B., Lang, D., Hillenbrand, R., Richter, M., Schachner, M. and Bartsch, U. (2003). Altered expression of CHL1 by glial cells in response to optic nerve injury and intravitreal application of fibroblast growth factor-2. *J. Neurosci. Res.* **71**, 835-843.

Rominger, C. M., Bee, W.-L. T., Copeland, R. A., Davenport, E. A., Gilmartin, A., Gontarek, R., Hornberger, K. R., Kallal, L. A., Lai, Z., Lawrie, K. et al. (2009). Evidence for allosteric interactions of antagonist binding to the smoothened receptor. *J. Pharmacol. Exp. Ther.* **329**, 995-1005.

Shen, F., Cheng, L., Douglas, A. E., Riobo, N. A. and Manning, D. R. (2013). Smoothened is a fully competent activator of the heterotrimeric G protein G(i). *Mol. Pharmacol.* **83**, 691-697.

Stanton, B. Z. and Peng, L. F. (2010). Small-molecule modulators of the Sonic Hedgehog signaling pathway. *Mol. Biosyst.* **6**, 44-54.

Stoppini, L., Buchs, P.-A. and Muller, D. (1991). A simple method for organotypic cultures of nervous tissue. *J. Neurosci. Methods* **37**, 173-182.

Street, C. A. and Bryan, B. A. (2011). Rho kinase proteins - pleiotropic modulators of cell survival and apoptosis. *Anticancer Res.* **31**, 3645-3657.

Thibert, C., Teillet, M. A., Lapointe, F., Mazelin, L., Le Douarin, N. M. and Mehlen, P. (2003). Inhibition of neuroepithelial patched-induced apoptosis by sonic hedgehog. *Science* **301**, 843-846.

Wang, S., Cesca, F., Loers, G., Schweizer, M., Buck, F., Benfenati, F., Schachner, M. and Kleene, R. (2011). Synapsin I is an oligomannose-carrying glycoprotein, acts as an oligomannose-binding lectin, and promotes neurite outgrowth and neuronal survival when released via glia-derived exosomes. *J. Neurosci.* **31**, 7275-7290.

Westphal, N., Kleene, R., Lutz, D., Theis, T. and Schachner, M. (2016). Polysialic acid enters the cell nucleus attached to a fragment of the neural cell adhesion molecule NCAM to regulate the circadian rhythm in mouse brain. *Mol. Cell. Neurosci.* **74**, 114-127.

Wright, A. G., Demyanenko, G. P., Powell, A., Schachner, M., Enriquez-Barreto, L., Tran, T. S., Polleux, F. and Maness, P. F. (2007). Close homolog of L1 and neuropilin 1 mediate guidance of thalamocortical axons at the ventral telencephalon. *J. Neurosci.* **27**, 13667-13679.

Yam, P. T., Langlois, S. D., Morin, S. and Charron, F. (2009). Sonic hedgehog guides axons through a noncanonical, Src-family-kinase-dependent signaling pathway. *Neuron* **62**, 349-362.